

The Two-Phase Screw-Type Engine with Flash Evaporation

Prof. Dr.-Ing. **K. Kauder**, Dipl.-Ing. **B. Kliem**

FG Fluidenergiemaschinen, Universität Dortmund

Deutsche Forschungsgemeinschaft (DFG) financially supported this project

Abstract

The two-phase screw-type engine is worth considering as an expansion engine in a trilateral-flash-cycle capable of utilising waste heat in the lower temperature range, because this kind of displacement engine is able to expand working fluids with a high proportion of liquid. Due to the low critical velocity and the blocked flow, the two-phase flow in the inlet of the screw-type engine has great influence on the quality of energy transformation. Less dissipation during the filling process can be expected in a system with rotating short nozzles, because the flash evaporation of the fluid will occur in the working chamber and not in the inlet port of the engine.

A flash evaporation test rig was installed. The evaporation of the nonsteady liquid jet is recorded by a video camera and a Xenon flash lamp. The cone angle of the atomized liquid jet is an index for the intensity of the flash evaporation. If the superheat attains 10 K, flash evaporation occurs. Above 27 K superheat the out-flow occurs in an "explosion-like" manner. Based on these investigations it is possible to design an improved inlet system.

1 Introduction

The two-phase screw-type engine was designed to use waste heat in the middle and lower temperature range. In a trilateral flash cycle this engine achieves better thermodynamic accessibility of the waste heat to the cycle, [1], [2]. Research work on the operational behaviour of this engine was performed at the City University London [2]. This was done mainly with organic working fluids. If water and steam are used as the working fluid, the filling process has a great influence on the quality of energy transformation [1], [3]. Two different filling systems and their influence on the energy transformation are described in [1]. The filling system with external atomisation feeds a conventional screw-type engine with wet steam through the inlet. Due to the low critical velocity of the wet steam, blocking flow occurs. The consequence is a reduction in pressure, with energy dissipation during the filling process. The second filling system consists of a disk with short nozzles, mounted on the high-pressure

side of the female rotor. The inlet nozzles are fitted in the middle of the tooth space area; Fig. 1. During a specific rotation angle, a connection

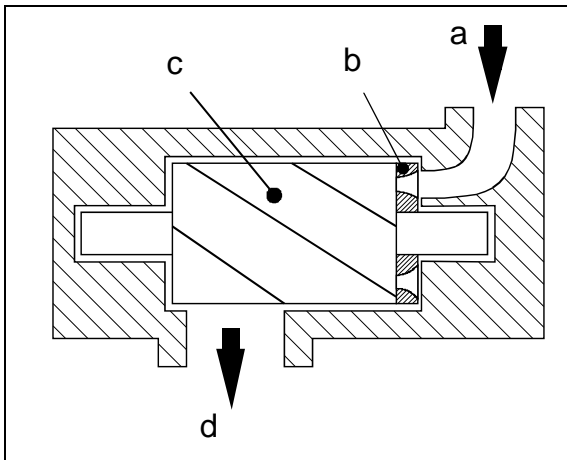


Fig. 1: *Filling system with rotating nozzles*

- a: hot water inlet*
- b :rotating nozzle disk*
- c: female rotor*
- d: wet steam outlet*

exists between the inlet and a tooth space nozzle. The flash evaporation of the hot water jet should occur first in the working chamber, if a short nozzle is used for filling. This presupposes an inlet pressure higher than the saturation pressure of the hot water. Lower energy dissipation during the filling process is to be expected with the second filling system.

First the filling system with rotating short nozzles is investigated independently of the engine to acquire information about the intensity of the flashing nonsteady liquid jet. The test-two-phase screw-type engine is presented in the perspectives section.

2 Theory of liquid jet break-up as a result of superheating

Flash evaporation should occur at the end of the short nozzle without any delay. Evaporation in the nozzles has to be avoided by selecting the right inlet pressure. At the nozzle exit the liquid jet should be atomised by partial evaporation of the superheated liquid.

The literature deals with experimental investigation of the atomisation of superheated liquid jets. These investigations have different objectives and refer to different test conditions [4], [5]. All investigations describe only a steady flow of the liquid jet. But the mechanisms depicted below are essential for an understanding of the processes involved.

2.1 Definition of superheating

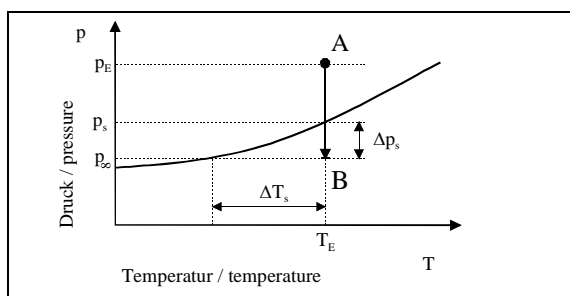


Fig. 2: *Change of state in the nozzle*

Superheating is a difference between the saturation temperature $T_{s(p)}$ in the thermodynamic equilibrium and the momentary temperature of the hot but not boiling liquid. Fig. 2 shows the change of state during the flow through a nozzle. At the nozzle inlet (state A) the pressure is

higher than the saturation pressure, which is supplied by the water temperature. During the acceleration of the liquid the pressure decreases. Because of the short process time, boiling does not occur. At the nozzle outlet (state B) ambient pressure p_∞ exists. The water is still in the liquid phase. Superheating depends on the temperature difference ΔT_s as shown in fig. 2. Super expansion Δp_s is the lower deviation of the saturation pressure $p_{s(T)}$. These deviations from the equilibrium state are decisive for the intensity of the phase transition.

2.2 Geometry of the jet break-up by flash evaporation

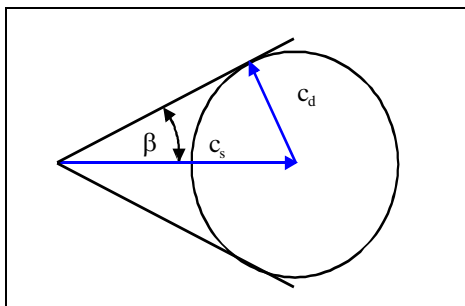


Fig. 3: Cone of the atomised liquid jet [5]

The cone angle β of the atomising liquid jet is the characteristic unit of the jet break-up in flash evaporation [5]. In a model the jet break-up is described as a superposition of the isentropic discharge velocity and the velocity of the jet expansion; fig 3. The velocity of the jet expansion c_d is given by:

$$c_d = \frac{\Delta p_s \rho'' d}{k \rho' \sigma} \quad \text{eq. (1),}$$

where ρ'' is the density of the steam, ρ' the density of liquid water, d the diameter of the nozzle and σ the surface tension. k is the jet constant, which is to be determined by experiment.

The isentropic discharge velocity c_s is given by:

$$c_s = \sqrt{\frac{2(p_E - p_\infty)}{\rho'}} \quad \text{eq. (2),}$$

where p_E is the inlet pressure and p_∞ is the ambient pressure.

These equations leads to the cone angle β :

$$\sin \beta = \frac{\Delta p_s \rho'' d}{k \sigma \sqrt{2 \Delta p \rho'}} \quad \text{eq. (3).}$$

The jet constant k depends on the geometry of the nozzle and the surrounding conditions. The cone angle of the atomising superheated liquid jet was measured at atmospheric pressure to verify this model. The nozzle diameter varied between 0.15 mm and 1.4 mm. The maximum superheat was 60 K. The value of the constant k in eq. (3) was calculated with the help of the measured angle β . The evaluation of [5] gives a value of 0.6 sm^{-1} for the constant k for 50 K superheating. Especially for larger diameter nozzles, superheating higher than 50 K triggers an explosion-like evaporation. With these conditions the observed cone angle does not correspond with eq. (3), but is much greater. The constant k involves the main influences on the intensity of flash evaporation such as the mechanisms of vapour nucleus growth and the vapour bubble growth. These experimental observations can be interpreted by the mechanism of boiling, described in [4]. A change in the constant k could be caused by a change in the nucleus formation.

3 Setup of the test rig and experimental performance

3.1 Flash evaporation test rig

Fig. 5 shows the setup of the test rig. A disk with nozzles (b) rotates in front of the hot water inlet. The dihedral angle of the nozzles is variable between 0° and 90° . The optical evaluation of the flashing liquid jet (c) is performed by a CCD video camera (d) through observation windows (e). The minimal exposure time is 10^{-5} s. The nozzle disk triggers a stroboscope.

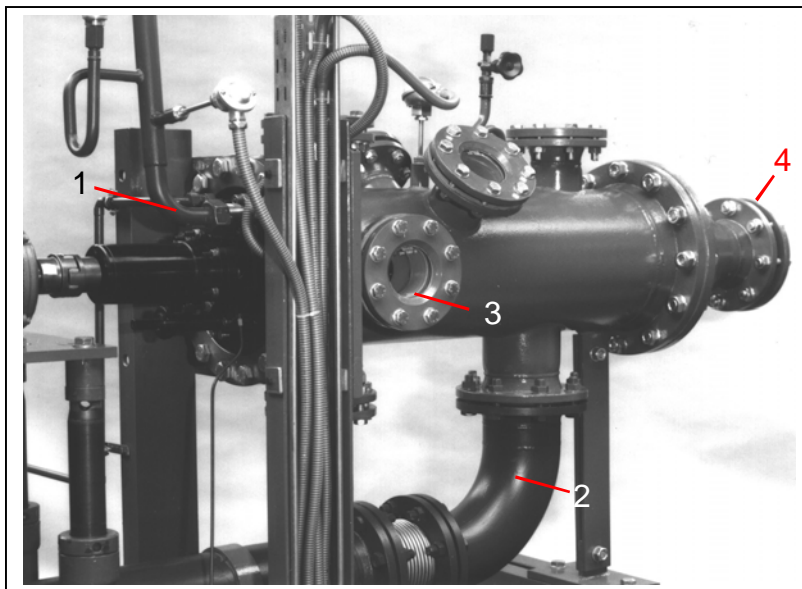


Fig. 4: *Test rig for the study of the rotating inlet system*

- 1 hot water supply pipe
- 2 wet steam pipe
- 3 observation window
- 4 lighting window

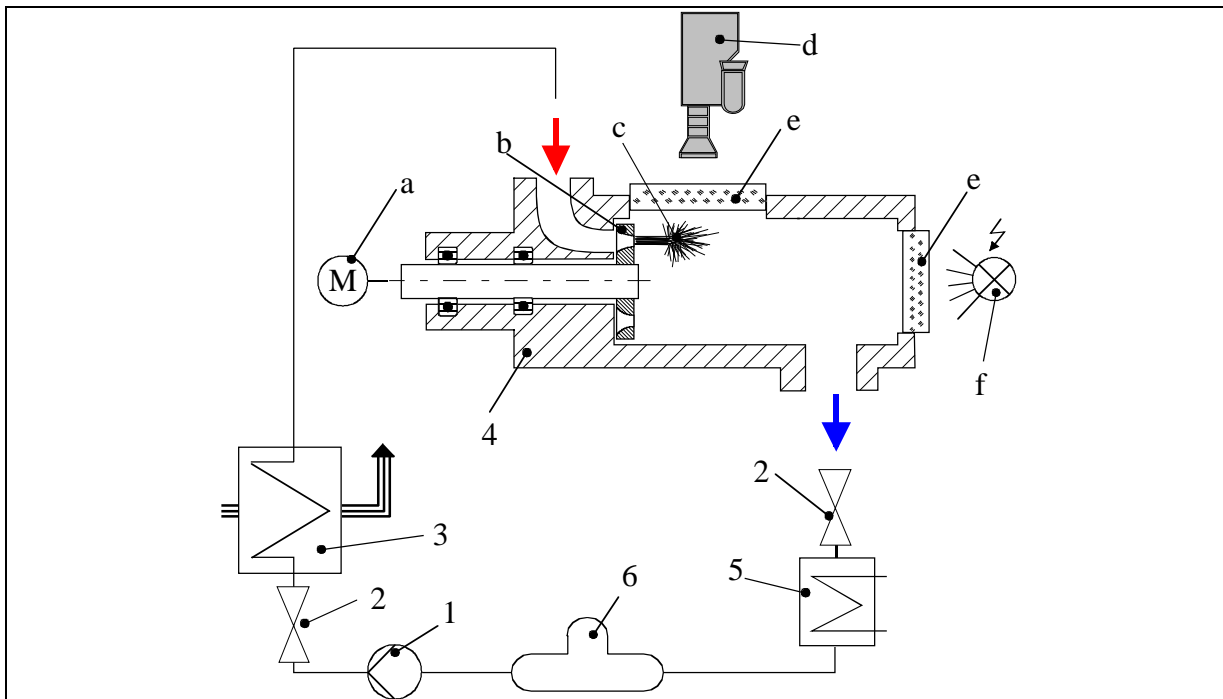


Fig. 5: Assembly of the test rig for the study of the rotating inlet system

The control unit can actuate a phase shift. A hot water boiler (3), fired with natural gas, provides the high pressure water. A throttle valve (2) and a speed controlled feed water pump (1) can regulate inlet pressure and mass flow. The maximum pressure of the test rig is 32 bar. A throttle valve in front of the condenser (5) inlet can control the pressure in the observation chamber. A programmable logic controller in connection with a PC is used for the data acquisition and the control of the test rig. Fig. 5 shows the test rig for the study of the rotating inlet system.

3.2 Contour of the nozzle

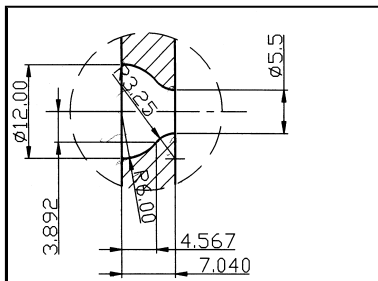


Fig. 6: Geometry of the tested short nozzle

A model for the calculation of the filling process with rotating short nozzles is given in [1]. The calculations are based on the design of the test two-phase screw-type engine. The inlet temperature is 188°C. This implies a nozzle outlet diameter of 7 mm. A connection between the inlet and the rotating short nozzle exists for a rotation angle of 62°. For nozzles with this diameter the mass flow is too high for the observation chamber as first experiments show. Droplets on the observation windows prevented

viewing. Due to this fact the outlet diameter of the nozzle was reduced to 5.5 mm. The geometry of the nozzle is given in fig. 6.

3.3 Experimental performance

The experimental investigation started with the observation of the steady liquid jet and its flashing. Therefore the nozzle disk was set at a rotation angle where there was a connection to the inlet. A constant operating level can be set with the help of the controlling unit of the hot water boiler and the speed control of the feed water pump. At first the observation chamber is at atmospheric pressure. Closing the throttle valve between observation chamber and condenser can raise the pressure nearly to the saturation pressure of the hot water. The air in the observation chamber escapes through an air-release valve. A reference picture of the observation chamber is taken before the series of tests starts to analyse the pictures of the flashing liquid jet.

The observation of the rotating flashing liquid jet is problematic. Strong vorticity causes a high amount of droplets on the observation windows. Due to this fact the maximal dihedral angle is limited to 20°. This reduces the mass flow and thereby the water spray on the observation windows.

4 Test evaluation

4.1 Steady jet atomisation

Fig. 7 shows a typical sequence of pictures of steady jet atomisation. The inlet pressure and temperature is nearly equal in all four pictures. The decreasing pressure in the observation chamber causes an increase in superheating and therefore an increase in the intensity of flash evaporation. The cone angle of the atomised liquid jet rises. To evaluate the test the cone angle is measured with the help of the pictures. This cone angle relative to superheating is shown in fig. 8. The inlet temperature of the water is 428 K, the inlet pressures are 9, 12 and 15 bar.

The curves are divided in to three characteristic areas:

Area I: $\Delta T_s < 9 \text{ K}$

A small amount of superheating has no influence on the jet spraying. The type of atomisation is the same as that for a “cold” liquid jet. In this area the cone angle rises with the inlet pressure. This is based on the higher turbulence in the liquid jet at higher flow velocity. The spraying of the jet in this area is shown in fig. 7a.

Area II: $9 \text{ K} < \Delta T_s < 27 \text{ K}$

The influence of evaporation starts at approx. 9 K superheating. The rise in of the cone angle, caused by increasing superheat, is larger for a low inlet pressure

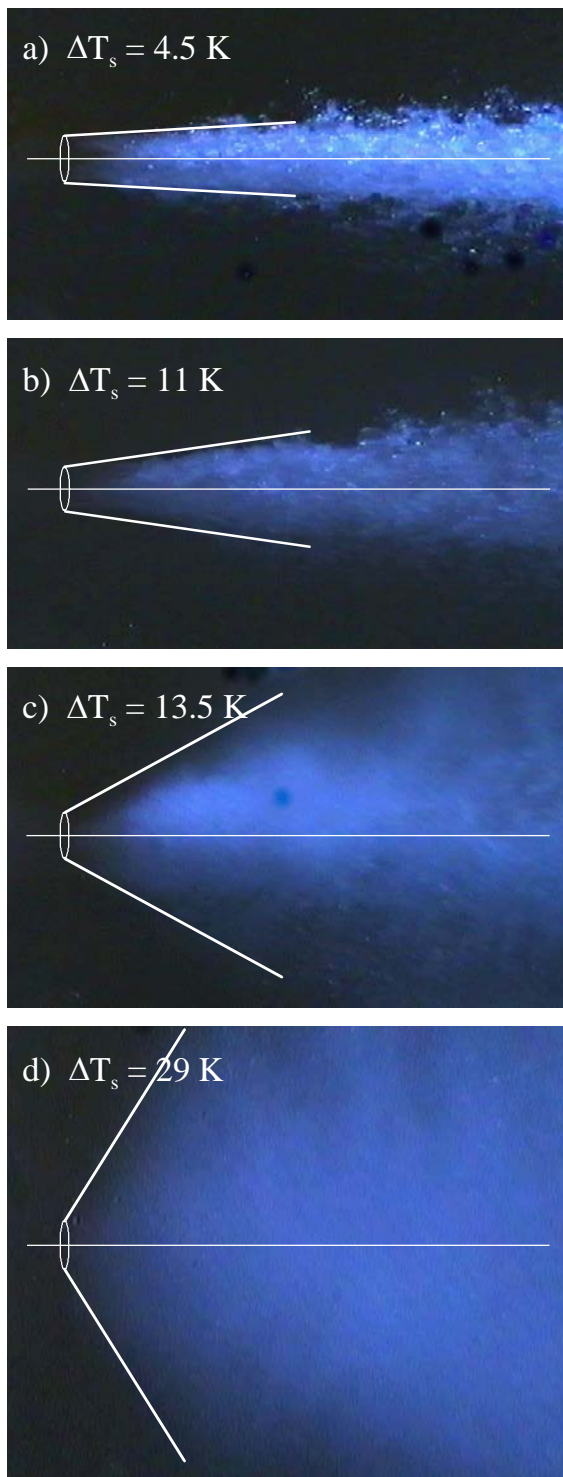


Fig. 7: *Atomization of the steady liquid jet inlet pressure: $p_E = 9$ bar, inlet temperature: $T_E = 428$ K $\Delta T_s =$ superheating*

than for a high inlet pressure. In the first approximation the growing velocity of the vapour bubbles is independent of the differential pressure between the inlet and the observation chamber, eq. 1. This explains the smaller cone angle for states of higher jet velocities combined with higher pressures. In area II all curves are convex. Fig. 8 also shows the curve of the constant k for the three inlet pressures. In area II the values for k are between 2.2 sm^{-1} and 2.9 sm^{-1} . These differences are moderate in this area, but it is still better to denominate k as a cone variable. It is conspicuous that in this area the curves of the three different pressures are close together.

Area III: $\Delta T_s > 27$ K

For superheat over 27 K the curves of the cone angle have a progressive gradient, as fig. 8 shows. An “explosive” atomisation of the liquid jet occurs. The large degree of superheat causes an intensified growth of the vapour nucleus as described in [4]. Theoretically one vapour bubble widens the jet in area II. In area III many nuclei accrue, so that the large number of vapour bubbles is responsible for a radial widening of the liquid jet. The interacting of the vapour bubbles causes a greater widening of the cone than calculated according to eq. 3, but eq. 1 is still correct. The value of the cone variable k decreases drastically in area III. Fig. 7 d shows the atomised liquid jet in this area.

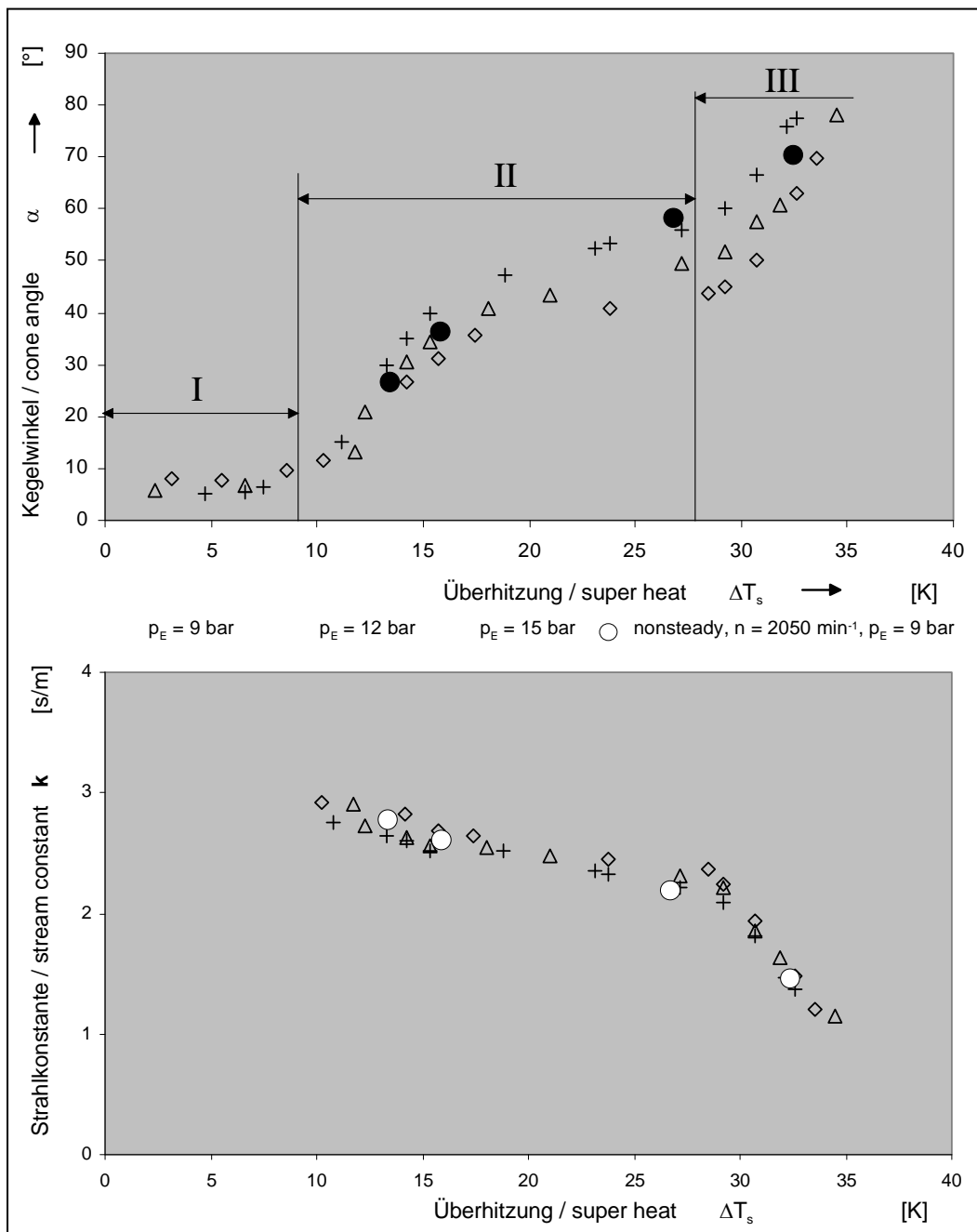


Fig. 8: Cone angle and stream constant versus superheat. Inlet temperature $T_E = 428 \text{ K}$

4.2 Rotating nozzle disk

The observation of the flash evaporation in the fluid jet is possible for dihedral angles up to 20° , otherwise the droplets on the window prevent observation. Fig. 9 shows a sequence at 2050 r.p.m. This number refers to 25 m/s as the tip speed of the male rotor in the test engine in [1]. The pictures of the sequences shown in fig. 9 are taken at different rotations with a different phase

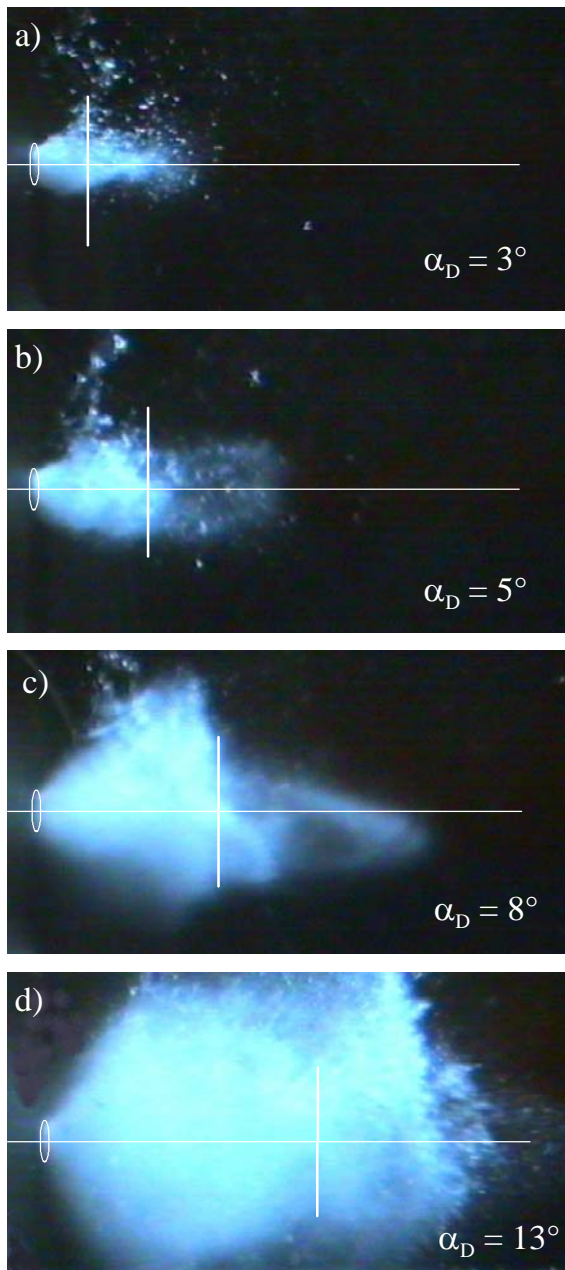


Fig. 9: Atomisation of the nonsteady liquid jet.

number of revolutions of the nozzle disk:
 $n = 2050 \text{ min}^{-1}$
 inlet pressure: $p_E = 9 \text{ bar}$,
 inlet temperature: $T_E = 428 \text{ K}$
 $\alpha_D =$ opening angle of the nozzle

angle, because just one picture per rotation can be taken. The theoretical position of a liquid particle can be calculated by using the isentropic discharge velocity (eq. 2), the dihedral angle and the rotation speed. The perpendicular lines in fig. 9 show where a liquid particle should be if it flows with isentropic discharge velocity at the

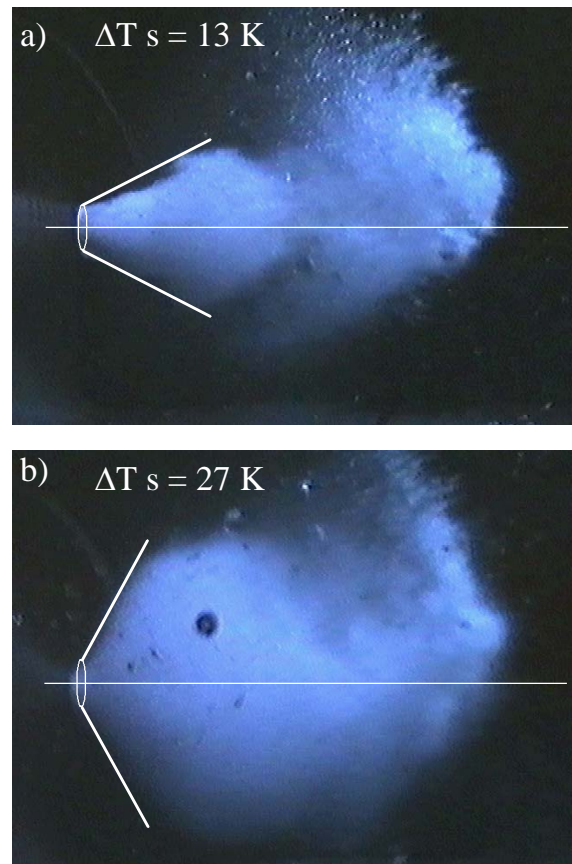


Fig. 10: Atomisation of the nonsteady liquid jet.

number of revolutions of the nozzle disk:
 $n = 2050 \text{ min}^{-1}$
 inlet pressure: $p_E = 9 \text{ bar}$,
 inlet temperature: $T_E = 428 \text{ K}$,
 opening angle of the nozzle: $\alpha_D = 13^\circ$,
 $\Delta T_s =$ superheating

beginning of the opening. It is noticeable that there is liquid in front of this perpendicular line. This is the result of leakage between the nozzle disk and the housing. The evaluation of the cone angle does not seem useful for dihedral angles lower than 10° because the jet atomisation could be affected by turbulence caused by redirection or flash evaporation. The dihedral angle of 12° indicates the end of the opening process. The liquid flow is directed from this angle. Fig. 10 shows the flashing behaviour of the nonsteady liquid jet with different degrees of superheating. The dihedral angle is 13° in both pictures. A distinct cone angle is visible. The cone angles of the nonsteady observations are also presented in the diagram in fig. 8. No major difference in the flashing behaviour of the steady liquid jet can be observed.

5 Perspectives

The injection of hot water into the expanding working chambers of the screw-type engine is a double nonsteady process. To achieve an intensive atomisation of the hot

			male rotor	female rotor
number of lobes	z	[-]	5	7
crown circle diameter	d_{KK}	[mm]	166	153
root circle diameter	d_{FK}	[mm]	102	89
length / diameter ratio	l/d	[-]	1,6	
maximal chamber volume	V_{max}	[m ³]	$0,673 \cdot 10^{-3}$	

Table 1: main parameters of the test two-phase screw-type engine

water, the difference between the inlet temperature of the hot water in the screw-type engine and the maximum saturation temperature during the filling process should not be lower than 15 K. For this setting a cone angle of 30° can be expected, as the visual investigation of the flash evaporation shows. The design of the test-engine is based on the results of these experimental investigations. The main parameters of the test two-phase screw-type engine are given in table 1. The engine has no

synchronisation gear. The bearings of the rotors are rolling contact bearings with water lubrication. This design completely avoids the need for oil circulation and sealing between the working chamber and the bearings. Fig 11 shows the female rotor with the mounted nozzle disk. For the indication of the engine six pressure transducers are installed. A general view of the test engine is given in fig 12. The test engine and an eddy current brake will be integrated into the hot-water test rig described in chapter 3. First trial runs are imminent.

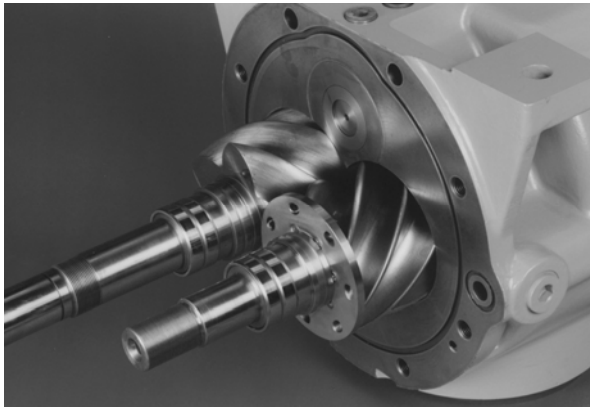


Fig. 11: *High-pressure side of the rotors. Female rotor with mounted nozzle disk*

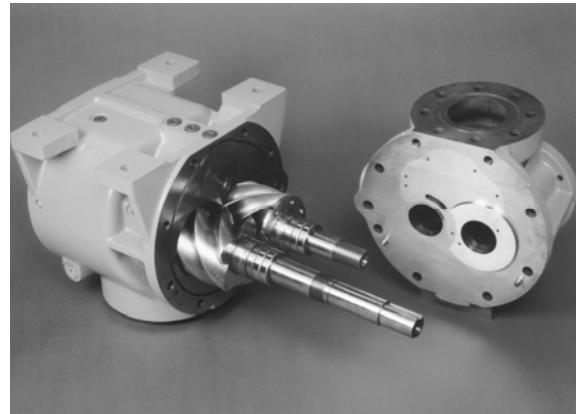


Fig. 12: *The test two-phase screw-type engine*

6 References

- [1] **Kauder, K. Kliem, B.** Zweiphasen-Schraubenmotor-Probleme des Füllvorganges. Two-phase screw type engine-Problems of the filling process. In: Schraubenmaschinen, Forschungsberichte des Fachgebietes Fluidenergiemaschinen Nr. 6, ISSN 0945-1870, S. 37 – 48, Universität Dortmund, 1998
- [2] **Smith, I. K. Stosic, N. Aldis, C. A.** Development of the trilateral flash cycle system. Part 3: the design of high-efficiency two-phase screw expanders. In: Journal of Power and Energy, Vol. 210, page 75 – 93, 1996
- [3] **Huster, A** Untersuchung des instationären Füllvorgangs bei Schraubenmotoren. Fortschritt-Berichte VDI Reihe 7 Nr. 336, Düsseldorf: VDI Verlag 1998
- [4] **Wildgen, A.** Untersuchung der Siedemechanismen im überhitzten Freistrah. Dissertation , TU München, 1985
- [5] **Polyaev, V. Kichatov, B. Boiko, I.** Outflow of Overheated Liquid Stream to the Atmosphere. In: High Temperature, Vol 36, No 1, pp. 98-101, 1998
- [6] **Skripov, V.** Metastable Liquids. Wiley, New York, 1974